Benefit of mesh adaption vs. conventional CFD approach for nacelle aerodynamics with ground effect

G.Millot†, S.Raynal and A.Laurencin
ALTRAN, Fluids & Thermal Engineering Expertise Center, 4, avenue Didier Daurat, 31700 Blagnac, FRANCE
† Email: gregory.millot@altran.com

ABSTRACT

The paper deals with nacelle aerodynamics during ground operations including crosswind effects with specific use of mesh adaption techniques to treat such configurations in CFD.
The development of UHBR (Ultra High Bypass Ratio) technology to increase the turbofan propulsive efficiency implies wider aircraft nacelles. If the conventional aircraft architecture is kept, it is needed to reduce ground clearance which enhances ground interactions during taxi and take-off phases. In particular a ground vortex may appear through the air intake for some combinations of wind speed, direction, and engine flow rate.

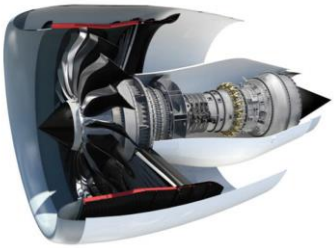

Figure 1. Concept of Ultra High Propulsive Efficiency (UHPE) demonstrator for short/medium range applications (Safran Aircraft Engines) [1].

Figure 2. Illustration of ground vortex during tests (NASA).

Such vortex can damage fan blades due to foreign object suction, dynamic loading and structural vibration. The ability to predict and characterize them during early design phases such as test bench is of huge interest to best design fan blades accordingly to potential ground vortices. Accurate numerical methods are necessary to characterize vortices on many configurations. This study analyses two approaches by comparing a conventional CFD software (ANSYS Fluent) with a specific solver integrating mesh adaptation techniques (ANASTAR, from LEMMA).
This takes place in InVIGO project realised on UHPE (Ultra High Propulsive Efficiency) in the framework of the Engine Integrated Technology Demonstrator (ITD) within the Clean Sky 2 programme.

1. INTRODUCTION

Ground effect on engine flow during ground operations have been largely studied for decades. Studies on ground vortices started in the 1950's with analytical and experimental analysis [2]. First papers highlighted the relationship between the size of the farfield sucked streamtube and the occurrence of ground vortices. When streamtubes intersect the ground, a ground vortex can rise from a stagnation point on the ground. This demonstrated the influence of Ui/Uinf (engine intake to wind velocity) ratio, that can be related to the sucked streamtube size relatively to the intake diameter. The influence of H/Di (engine axis height to fan plane diameter ratio) was also highlighted since it governs the possible interaction between streamtube and ground.
Until 2000's, most studies were experimental. They globally agree on similar trends regarding limit between vortex and no vortex cases.

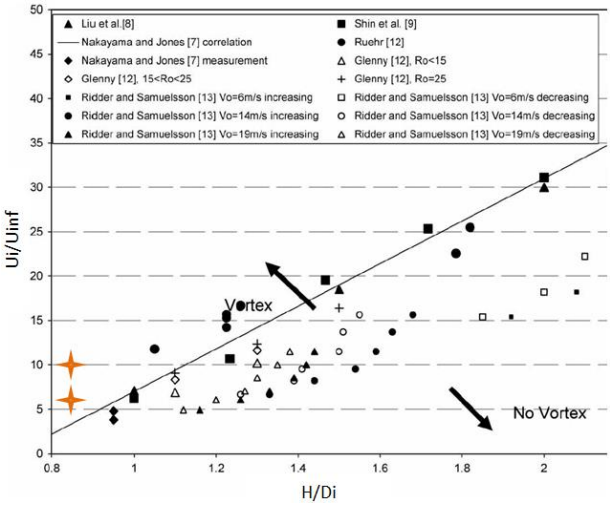

Figure 3. Vortex/No Vortex limit based on several studies (adapted from [3]). Orange crosses corresponding to the cases studied here confirm the vortex expectations.

Since 2000's, new CFD studies tackled the vortex simulation topic and were generally in agreement with experimental data. Many software have been used with either RANS, URANS or LES approach. Most of them have static mesh with less than 10 million elements and most recent studies used a 20 million element mesh.
In the current paper, two numerical approaches with steady calculations are compared. On the one hand, ANSYS Fluent is used with a rather fine mesh to accurately capture vortex characteristics. On the other hand, ANASTAR software developed by LEMMA is used to assess the potential gain due to mesh adaptation techniques. The main configuration tested is a ground vortex case with Ui/Uinf = 10 and H/Di = 0.85. The combination of these two parameters ensured the vortex presence as agreed in literature (see Figure 3) [4]. An additional configuration is tested with outlet nozzles for core and bypass flows. For this case, Ui/Uinf is changed to 6.
First of all, numerical approaches and mesh strategy used with each solver will be described. Then, results will be described with specific focus on vortex characteristics.

2. NUMERICAL SET-UP

2.1. Geometry

For each configuration, Fluent and ANASTAR runs have the same geometry. The simplified engine geometry is at the center of a large cylindrical domain with 50 m radius and 38 m height. Bottom of cylinder is considered as ground. Vertical position of engine relatively to ground directly sets the H/Di ratio.

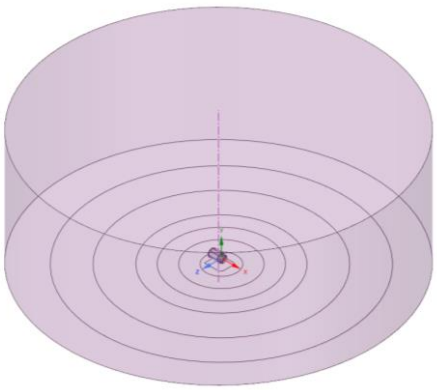

Figure 4. Domain of calculation

Two simplified engines have been built with a generic nacelle geometry. Its main characteristics at full scale are maximum external diameter = 1.3 m, fan plane diameter Di = 1.047 m, nacelle length = 3.5 m. No internal parts are modelled except for spinner geometry with a round shape and a 0.288 m radius. Engine intake is set inside nacelle by extruding fan plane geometry along 1 Di distance.
For ground vortex case, the geometry is set at model scale (1/7.07 ratio) for future comparison with experiments. Nacelle outlet is simplified with a planar back face without flow.

The second configuration comprising outlet nozzle is a more complex engine geometry. Global nacelle geometry and spinner are the same but the nacelle outlet is complexified so that core flow and bypass flow can be numerically imposed. There are no link between sucked flow inside engine and released flow at nozzle outlets. Primary and secondary nozzle throat area are 0.2014 m² and 1.7632 m², respectively.

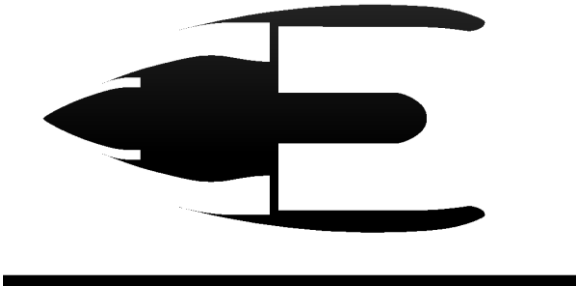

Figure 5. Vertical cut of engine geometry above ground with rear nozzles

2.2. Mesh for Fluent

Meshes for ANSYS Fluent runs are generated with ANSYS Meshing software. Meshes are built for Low-Reynolds turbulence modelling at wall. They are composed with tetrahedral elements, with 20 prisms layers on nacelle walls, and 15 layers on ground, to reach Y+ < 2 on walls. Nacelle walls are refined with a 12° curvature criterion with several surface sizing. Five bodies of influence are also set for volume refinement, specifically in ground vortex region. For case with outlet nozzle, three other conic bodies of influence are put in the engine rake to allow accurate solving of fluid mixture layers and interaction with ground.
Meshes for these two cases counts 44 and 78 million elements, respectively. This allows having at least 10 cells in the ground vortex diameter, more than 70 tetrahedral cells in the fan plane diameter, and 20 tetrahedral in both nozzle throat sections. All meshes have good quality with skewness below 0.9 for all cells and orthogonal quality above 0.1 for tetrahedral. A convergence study has been performed for case without outlet nozzles which confirmed these sizings.

2.3. Mesh for ANASTAR

Mesh process for ANASTAR runs is much different. The ANASTAR suite, which is developed by LEMMA, is focused on solvers with automatic remeshing functionalities supporting anisotropic tetrahedral cells [5]. The automatic remeshing process starts from a full tetrahedral coarse mesh generated by the user. In the present cases, the order of magnitude of starting meshes varies between 100 000 and 1 000 000 elements, only based on a minimum and maximum cell size and a proximity criterion to have 5 cells in all gaps.

From these meshes, runs are performed sequentially with increasing mesh size, until measured quantities are converged. The criterion for local refinement used here

is velocity gradient. No user input is required, the solver automatically adjust cell size based on its calculations. Each sub-run has a maximum number of 1000 iterations and can stop earlier if monitored forces are converged.

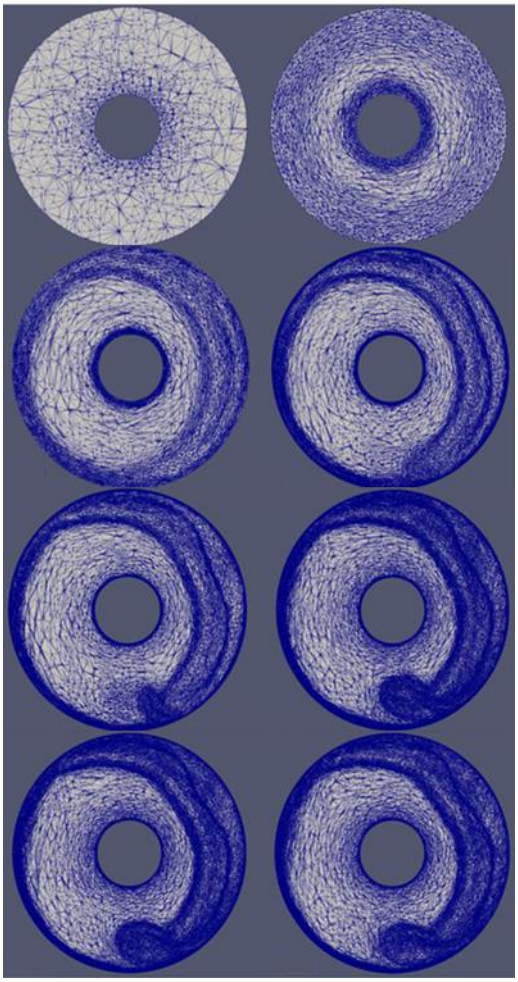

Figure 6. Increasing mesh resolution (left-right then top-down) in fan plane

Final meshes are much different from starting ones with strong anisotropy. Therefore, cells in region with a dominant flow direction with low gradient in this direction are often flattened. Cells in far region have large size, whereas boundary layers are much refined. Cells in region with large gradient, such as ground vortex, intake detachment or interaction between nozzle outlet flow and side wind, are then automatically refined.

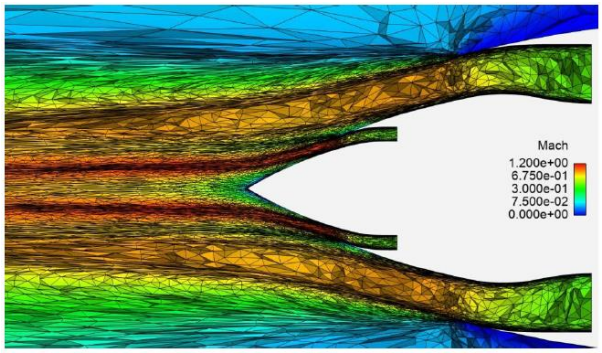

Figure 7. Automatic mesh refinement in nozzle outlets colored by Mach number.

Final mesh for ground vortex case comprises 12 million elements. Case with outlet nozzle shown in this paper also comprise 12 million elements but was stopped early in the mesh convergence process. More iterations could have been required.

2.4. Solver settings for Fluent

ANSYS Fluent solver has been chosen as state-of-the-art reference and common practices for aerodynamics calculations have been applied here.
Pressure-based double precision solver is used with 2nd order spatial schemes and steady formulation. k-ω SST turbulence model is applied and compressible flow is used.
Ground and nacelle walls are conditioned as non-slip walls. Engine intake is set as pressure outlet with target mass flow rate. The circular side of the global domain is set as velocity-inlet with 90° direction from engine axis. The top global domain surface is set as pressure outlet with 101325Pa static pressure and accounts for the pressure reference for the calculation.
Flow rates and temperatures imposed at engine are described for each run in Table 1. Most properties have been estimated with an in-house whole engine model software to approach Take-Off rate for UHBR engine type. Difference between inlet and outlet flow for outlet nozzle case was not intentional and due to encountered difficulty with ANASTAR to precisely impose conditions. This does not impact the zone of interest at engine outlet.

Case	Boundary	Mass flow rate (kg/s)	Total temperature (K)
Ground vortex	*Intake flow*	230	-
Nozzle	*Intake flow*	450	-
	Outlet core flow	55.15	856.73
	Outlet bypass flow	561.44	331.93

Table 1. Engine boundary conditions

Runs are initialized with a simplified solution calculated by Fluent based on boundary conditions, by using the combination of a hybrid initialization followed by a Full Multi-Grid initialization.
The run for first configuration with focus on ground vortex is the most complicated to monitor efficiently. Specific techniques mainly based on Q-criterion allowed extracting ground vortex position and strength during the whole run. A convergence strategy allowed reaching oscillating but stable vortex position and strength, with good mass flow balance and pressure convergence. A total of 10 000 iterations were performed. Same strategy was applied for run with outlet nozzles.

2.5. Solver settings for ANASTAR

Solver settings for ANASTAR runs followed LEMMA recommendations and requirements for the automatic remeshing process. Third order spatial scheme is implemented for all variables and Spalart-Allmaras turbulence model is applied. Incompressible flow has been chosen for ground vortex case, and compressible

formulation is applied for case with high speed in nozzle outlets.

Some points differ from ANSYS Fluent settings but applying best solution for each software has been favoured over applying exactly the same method. Indeed, Fluent third order spatial scheme has not been applied since it is generally less conservative, and Spalart-Allmaras model is currently recommended for automatic remeshing with ANASTAR whereas Fluent shows better physics modelling with k-ω SST model.

Most boundary conditions are the same as Fluent. Engine intake needs distinct approach in incompressible runs using a velocity inlet with outward direction. Velocity is estimated based on target mass flow rate, ambient pressure, density and temperature. In compressible runs, nozzle outlets are defined with velocity, pressure and temperature values. ANASTAR showed difficulties in imposing the exact velocity value. Fluent runs are based on the effective ANASTAR mass flow rates.

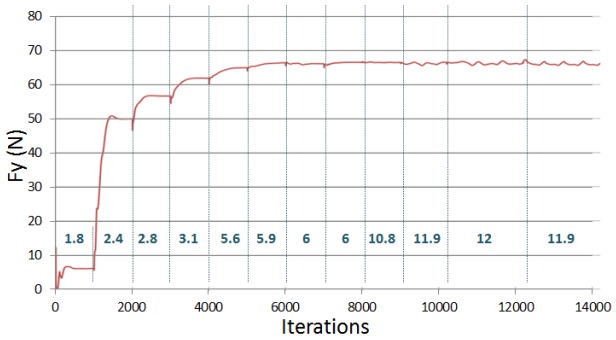

Figure 8. Suction force on ground along sub-runs with corresponding mesh size (in million elements) at the bottom for ground vortex case

First run on gross mesh is initialized with no flow and ambient pressure and temperature. CFL maximum values are set as 1 and 10 for diffusive and convective CFL respectively. Forces on ground below nacelle intake and on nacelle lip are monitored and used to define whether a sub-run is converged. For each sub-run, the maximum number of iteration was set to 1000.

3. RESULTS

3.1. Mesh comparison

Following figure compares meshes in the vertical fan plane.

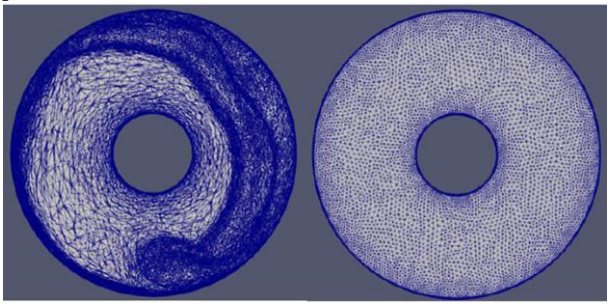

Figure 9. Mesh in vertical fan plane for final ANASTAR run (left) and Fluent (right)

Fluent mesh (right) is mainly homogeneous, with refinements near walls. At the end of sequential calculation, ANASTAR mesh (left) is strongly heterogeneous with very refined mesh in the flow detachment and in the vortex region at the bottom of the plane. Boundary layers are also refined. Nonetheless, in main zones, cells are flattened and are much refined in the radial direction since low variations occur azimuthally far from detachment and vortex.

For the second case, boundary and mixing layers are much refined. As seen with first case, cells are refined radially and remain relatively large in other directions.

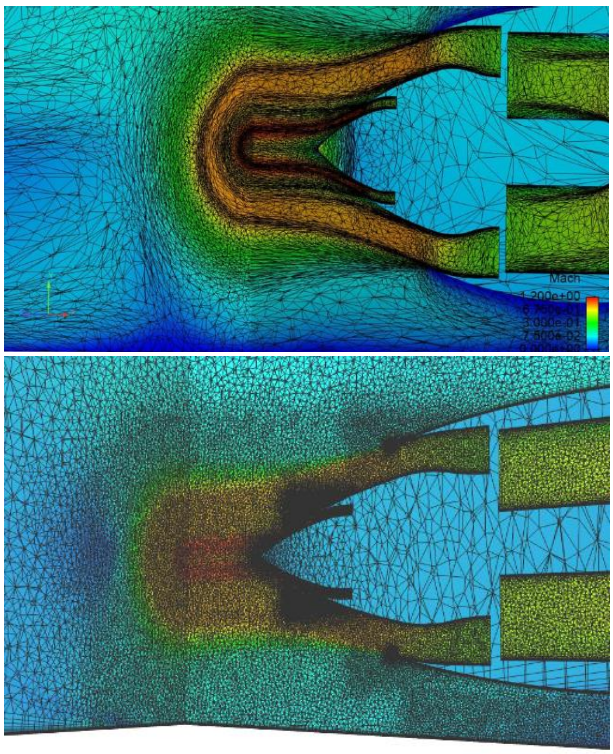

Figure 10. Visualization of the jet at nozzle exhaust with ANASTAR (top) and Fluent (bottom) – Mach number on mid-vertical plane & normal plane 1m downstream the plug tip

3.2. Vortex characteristics

Some vortex characteristics have been analysed for ground vortex case with each solver. Three criteria have been calculated: vortex center position, radius and strength.

First step is extracting a relevant but gross vortex by using iso Q-criterion. By looking at total pressure or vorticity fields, a Q-criterion value is defined and a rather circular sub-surface is extracted. By averaging coordinates on this sub-surface, vortex center is defined.

Vortex radius and strength are calculated by post-processing vorticity fields. Vortex radius is commonly calculated by looking for radius with maximum tangential velocity. Concentric disc with increasing r radius are generated from vortex center and vorticity component normal to vertical plane is integrated. Thanks to Stokes relation, the integral of vorticity over each disc with r radius can be related to tangential velocity Vtheta(r) along disc external perimeter.

$$\oint_{\partial S} \vec{V} \cdot \mathrm{d}\vec{l} = \iint_{S} \overrightarrow{\mathrm{rot}}\, \vec{V} \cdot \mathrm{d}\vec{S}$$

The maximum value of Vtheta(r) determines the vortex radius. Figure 11 below compares Vtheta(r) as a function of r for ground vortex runs. Fluent and ANASTAR results are very close with resulting vortex radius around 0.12 m.

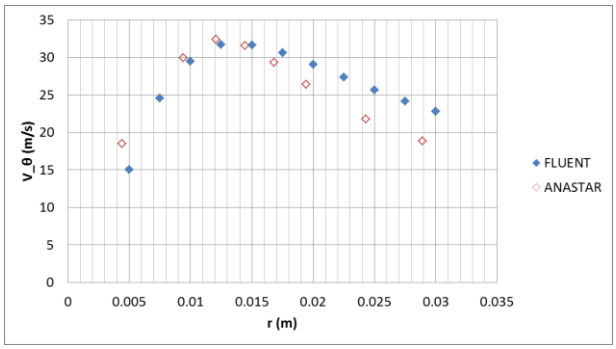

Figure 11. Vtheta as a function of given vortex radius for Fluent and ANASTAR.

Figure 12 plots the vortex center with this radius on a vertical fan plane.

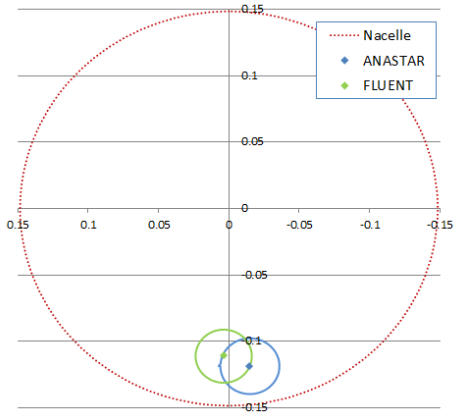

Figure 12. Vertical fan plane with Fluent and ANASTAR vortex position and radius at the bottom.

3.3. Results

Figure 13 compare vorticity fields in the fan plane. Global features are very similar, although Fluent calculation predicts higher vorticities at the vortex center. This can be related to Spalart-Allmaras turbulence model which is more diffusive than k-ω SST.

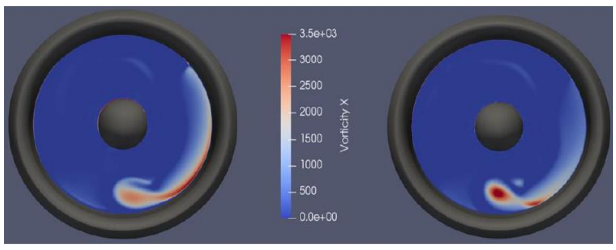

Figure 13. Axial vorticity in the fan vertical plane for ANASTAR (left) and Fluent (right)

Figure 14 shows an isocontour of Q-criterion. Ground vortex and flow detachment are well captured with such criterion. Both runs show very similar trends.

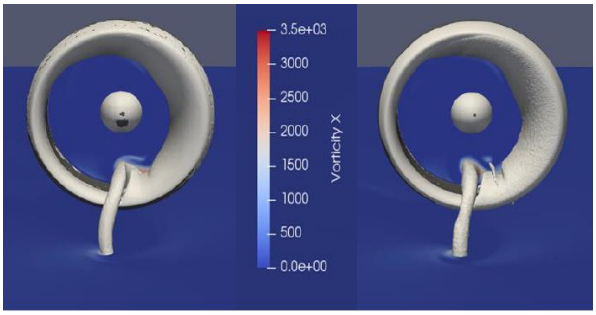

Figure 14. Isocontour of Q-criterion to vizualize vortex and detachment for ANASTAR (left) and Fluent (right).

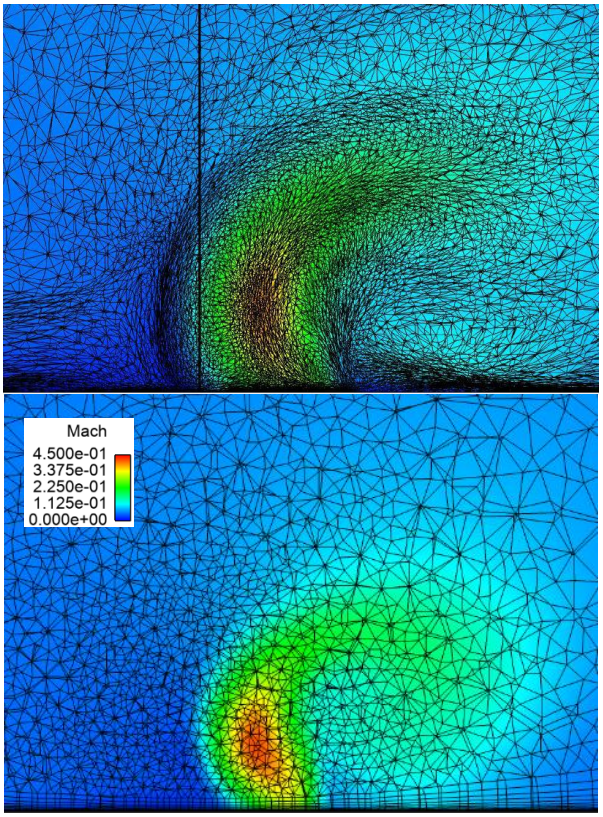

Figure 15. Visualization of the jet with ANASTAR (top) and Fluent (bottom) – Mach number on a normal plane 16m downstream the plug tip

Figure 15 compares Mach contours and meshes 16m downstream of the plug tip. Mesh generated for Fluent is relatively gross at this position with common expansion mesh ratio and volume refinements. Adapted mesh with ANASTAR is much refined on the ground and in mixing layers. Within core flow, ANASTAR mesh is 5 to 10 times more refined in the lateral (i.e. wind) direction. Although Fluent captures global features, it seems that the diverted plume is best resolved with ANASTAR with less diffusion. The mesh adaption capability can be appreciated since gradient zones are well refined whereas outside jet effect cell size is quite similar than on the Fluent mesh. Similar observation can be made on Figure 10 in which mixing between flows is less pronounced with ANASTAR run.

The wind/jet interaction is illustrated with top view on

the Figure 16. Global behaviour is quite similar but it is clear that jet diffusion is stronger on Fluent computation, inducing a more bended wake far from the exhaust (loss of dynamics effect)

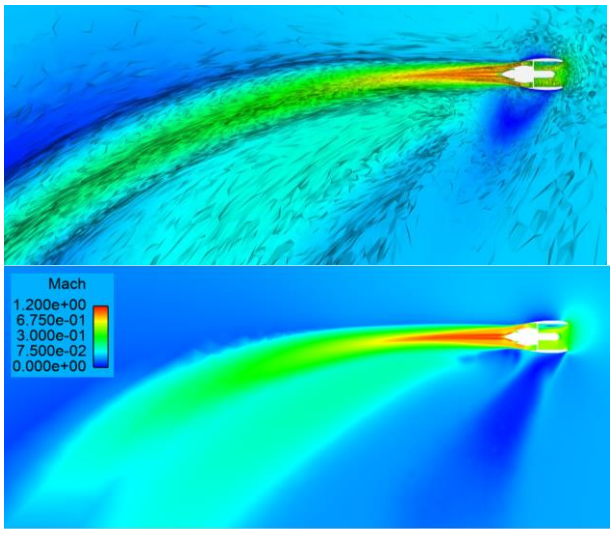

Figure 16. Visualization of the jet with ANASTAR (top) and Fluent (bottom) – Mach number on a cut plane parallel to the ground at the engine axis position

4. CONCLUSION

This study investigated the potential benefit of automatic remeshing capabilities for problematics related to nacelle aerodynamics in ground conditions.
ANASTAR software has such capabilities and was compared to more conventional ANSYS Fluent software.
First case dealt with ground vortex, for which small features with large vorticity need to be captured. For this configuration, both simulations showed very similar results. Total mesh size and CPU time with ANASTAR were about 4 times smaller than Fluent run. This clearly gives interest to automatic remeshing approach. However, wind and engine velocities were rather low, and the precision and benefit with ANASTAR would require to be confirmed with more challenging velocities (such as 200 m/s engine intake with 20 m/s cross-wind) where unsteadiness is more present.
Second case added outlet nozzles with large outlet speeds and jet interaction with cross-wind. Mesh adapted by ANASTAR was mainly refined in mixing layers. Most significant differences between Fluent and ANASTAR were located far from engine where Fluent mesh become coarser. In this area, the plume is up to 10 times much refined with ANASTAR, even if the entire mesh remains 6 times smaller than that used with Fluent. In such a case, it is very difficult to properly define mesh refinement *a priori*. In addition, the location which would require it depends on the operating point so that important engineer time would be needed to perform global characterization.

In conclusion, the automatic remeshing approach investigated here with ANASTAR shows interesting results with much smaller mesh and CPU time. All the benefits would need to be more deeply investigated on other design points with closer look to turbulence and unsteady phenomena. All or part of this approach could be used on a large range of industrial configurations with many other topics requiring fluid simulations with strong local gradients.

5. ACKNOWLEDGEMENT

The project leading to this application has received funding from the Clean Sky 2 Joint Undertaking under the European Union's Horizon 2020 research and innovation program under grant agreement No [864288].
This communication and the data provided here represent only the authors' view and do not engage Clean Sky 2 nor the European Union for any use that may be made of the information they contain.

We would also like to thank Safran Aircraft Engines and CSTB for their involvement on this project.

6. REFERENCES

[1] Brouckaert, J. F., Mirville, F., Phuah, K., & Taferner, P. (2018). Clean Sky research and demonstration programmes for next-generation aircraft engines. The Aeronautical Journal, 122(1254), 1163-1175.

[2] Rodert L. A. & Garrett F. B. (1953). Ingestion of foreign objects into turbine engines by vortices. NACA TN 3330, National Advisory Committee for Aeronautics

[3] Jermy, M. & Ho, W. (2008). Location of the vortex formation threshold at suction inlets near ground planes by computational fluid dynamics simulation. Proceedings of the Institution of Mechanical Engineers Part G Journal of Aerospace Engineering (pp. 393-402).

[4] Murphy, J. (2008). Intake ground vortex aerodynamics. PhD Thesis, Cranfield University, Cranfield.

[5] Loseille, A., Dervieux, A., Alauzet, F. (2010). Fully anisotropic goal-oriented mesh adaptation : 3D anisotropic mesh adaptation for functional outputs. IV European Conference on Computational Mechanics, ECCM2010. Palais des Congrès, Paris, France, May 16-21, 2010.